GEOPHYSICAL RESEARCH LETTERS, VOL. 24, NO. 5, PAGES 595-598, MARCH 1, 1997

Simultaneous observations of Polar Stratospheric Clouds and HNO_3 over Scandinavia in January, 1992

Steven T. Massie, James E. Dye, Darrel Baumgardner, William J. Randel, Fei Wu, XueXi Tie, Liwen Pan, Francois Figarol, and Guy P. Brasseur

National Center for Atmospheric Research, Boulder, Colorado

Michelle L. Santee and William G. Read

Jet Propulsion Laboratory / California Institute of Technology, Pasadena, California

Roy G. Grainger and Alyn Lambert

Atmospheric, Oceanic and Planetary Physics, Oxford University, Oxford, UK

John L. Mergenthaler

Lockeed-Martin Research Laboratory, Palo Alto, California

Azadeh Tabazadeh

NASA-Ames Research Center, Moffett Field, California

Abstract. Simultaneous observations of Polar Stratospheric Cloud (PSC) aerosol extinction and HNO_3 mixing ratios over Scandinavia are examined for January 9-10, 1992. Data measured by the Microwave Limb Sounder (MLS), Cryogenic Limb Array Etalon Spectrometer (CLAES), and Improved Stratospheric and Mesospheric Sounder (ISAMS) experiments on the Upper Atmosphere Research Satellite (UARS) are examined at locations adjacent to parcel trajectory positions. Regression coefficients, obtained from Mie calculations, are used to transform aerosol extinctions into aerosol volume densities. Graphs of volume density versus temperature, and importantly, HNO_3 mixing ratio versus temperature, show volume increases and simultaneous loss of HNO_3 as temperatures decrease. The data is consistent with initial PSC growth processes which transform sulfate droplets into ternary droplets or nitric acid dihydrate (NAD) particles.

Introduction

The availability of satellite data, measured daily and globally, makes possible studies of the formation and dissipation of Polar Stratospheric Clouds (PSCs) along parcel trajectories. This letter develops and applies such techniques to the data measured by the Upper Atmosphere Research Satellite (UARS). UARS instruments simultaneously observe both aerosol extinction and gas phase HNO_3, and thus it is possible to study the interconversion of gas phase HNO_3 into PSC particles.

PSCs are thought to be composed of ice crystals (Type II), nitric acid trihydrate (NAT) solid particles (Type Ia), ternary solution ($HNO_3/H_2SO_4/H_2O$) droplets (Type Ib), and metastable (HNO_3/H_2O) particles (Type Ic). Studies of forward scattering spectrometer probe (FSSP), balloonborne backscattersonde, and lidar data, have indicated the presence of ternary, NAT, and metastable particles (*Tabazadeh et al.*, 1994a, *Tabazadeh et al.*, 1996, *Carslaw et al.*, 1994, *Drdla et al.*, 1994, *Larsen et al.*, 1996).

Simultaneous UARS observations of aerosol extinction, measured by the Cryogenic Limb Array Spectrometer (CLAES) and Improved Stratospheric and Mesospheric Sounder (ISAMS) experiments, and gas phase HNO_3, measured by the CLAES and Microwave Limb Sounder (MLS) experiments, are used to study the formation of a Polar Stratospheric Cloud (PSC) over Scandinavia during January 9-10, 1992. UARS observations on January 9 and 10 are used only if they are adjacent to specific parcel trajectories. The parcel positions originate over Greenland on January 9, and then proceed to a region of cold temperature, low HNO_3, and high aerosol extinction, located over Scandinavia on January 10.

The UARS extinction data are transformed into volume density values using regression coefficients, obtained from Mie calculations. Graphs of volume density versus temperature, and gas phase HNO_3 versus temperature, reveal the interconversion between the gas and aerosol phase. The data are compared to equilibrium, and time dependent calculations, for PSCs of several compositions.

UARS Data

This study uses UARS observations at 46 and 68 hPa. CLAES and ISAMS aerosol extinction precisions and accuracies for this range of pressure are on the order of 20 and 35% (*Massie et al.*, 1996, *Lambert et al.*, 1996). *Kumer et al.* (1996) discuss the CLAES (version 7) data, and *Santee et al.* (1996) discuss the MLS (version 4) HNO_3 data, which are accurate to 2 and 3 ppbv, respectively, at 46 hPa. MLS data at 68 hPa are obtained by interpolation of 46 and 100 hPa retrieved measurements.

Since PSC microphysics is quite temperature dependent, it is important to assess the accuracy of the United Kingdom

Paper number 97GL00315.
0094-8534/97/97GL-00315$05.00

Meteorological Office (UKMO) temperatures used in this study. Using the methodology of *Manney et al.* (1996), comparisons between 1311 UKMO and radiosonde temperatures at pressures near 46 hPa for January 1-14, 1992 show that the UKMO temperatures are 1 K warmer than the radiosonde temperatures for the Arctic, with an rms deviation of 2 K about the bias. UKMO temperatures were therefore decreased by 1 K.

To transform the UARS extinction data into volume densities, Mie calculations are used to establish linear regression coefficients for each of the CLAES and ISAMS observational wavelengths. The Mie calculations use Arctic FSSP particle size distributions measured during the AASE II flights of the ER-2 (*Dye et al.*, 1992) and sulfate aerosol size distributions measured over Laramie, Wyoming (*Deshler et al.*, 1993). The FSSP data set contains size distributions for ternary solution droplets, sulfate droplets (at temperatures greater than 200 K), and NAT particles. Regression coefficients were established for several sets of refractive indices (e.g, HNO_3/H_2O, H_2SO_4/H_2O and NAT) for various weight concentrations of HNO_3 and H_2SO_4. Binary HNO_3/H_2O indices approximate the $HNO_3/H_2O/H_2SO_4$ ternary indices, since the weight percent of H_2SO_4 is small in a ternary droplet for temperatures less than 195 K. For each extinction data point, the weight percent of H_2SO_4 and HNO_3 is calculated, the composition is specified to be either sulfate, ternary or NAT, and the appropriate set of regression coefficients are then used to transform extinction to volume density. Details of the transformation calculations are discussed elsewhere (*Massie et al.*, manuscript in preparation).

UARS Data on January 9 - 10

Plate 1 displays mapped UKMO temperatures (decreased by 1K), CLAES HNO_3 mixing ratios, and ISAMS 12.1 μm extinction data, on the 460 K potential temperature surface for January 10, 1992. Low mixing ratios and high extinction values are associated with a region of cold temperature over Scandinavia

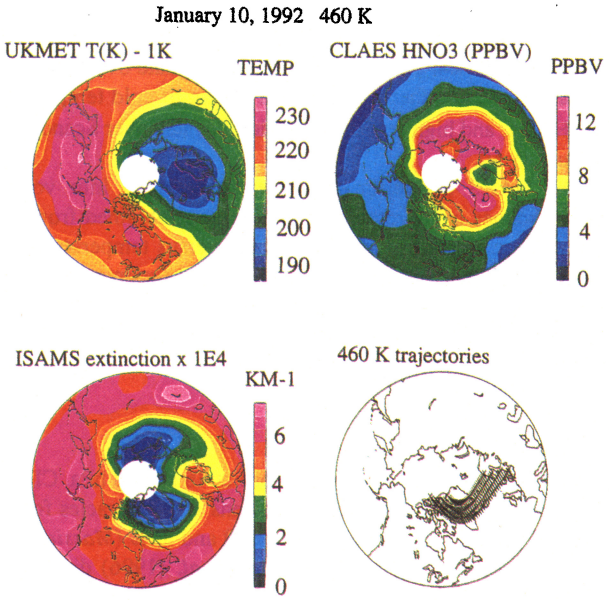

Plate 1. Maps of UKMO temperature (K), CLAES gas phase HNO_3 (ppbv), and ISAMS 12.1 μm extinction (10^{-4} km^{-1}) for January 10, 1992 on the 460 K potential temperature surface. Parcel positions are over Greenland on January 9, and over Scandinavia on January 10.

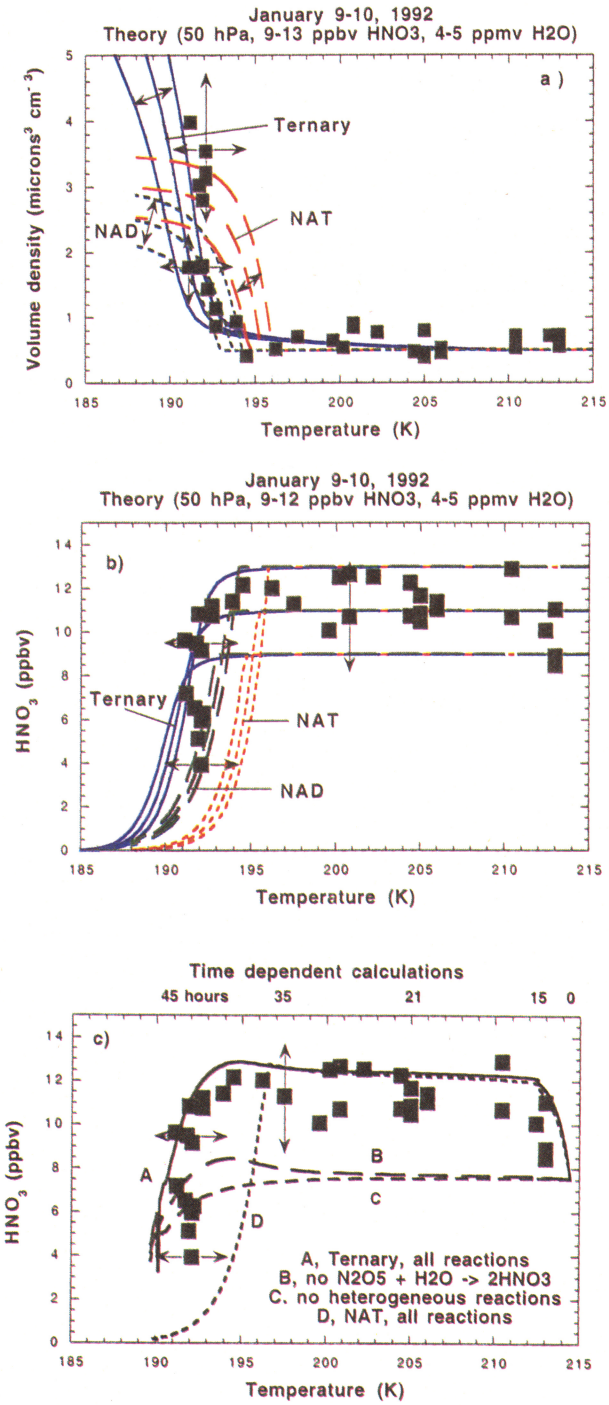

Figure 1. Profile data which are adjacent to parcel trajectory positions on January 9 and January 10, 1992. a) Average values of ISAMS and CLAES volume densities. b) Averaged CLAES and MLS HNO_3 mixing ratios which correspond to the data points in Figure 1a. c) Time dependent HNO_3 mixing ratios, calculated with and without heterogeneous reactions.

(see Figure 3 of *Taylor et al.*, 1994, for maps of temperature and aerosol extinction on adjacent days). Also displayed are specific parcel trajectories, calculated using UKMO wind field data. The parcels are located on the 460 K surface (corresponding to 19 - 20 km altitude over Scandinavia). Westernmost parcel positions, located over Greenland on January 9, have temperatures near 215 K, and easternmost positions over Norway on January 10 have temperatures near 190 K.

The volume densities presented in Figure 1a are an average of nine volume densities derived from ISAMS 12.1, 6.23 μm, CLAES 12.82, 12.66, 11.86, 11.36, 10.81, 7.96, and 6.23 μm extinction data. UARS aerosol extinction and HNO_3 data at 46 and 68 hPa were linearly interpolated in pressure, to the pressure value of the nearest parcel trajectory point. The assigned temperature is that of the nearest trajectory point. Horizontal arrows indicate the ±2 K rms deviation between the UKMO temperatures and that of the radiosondes. Vertical error bars are rms differences between the graphed averages and the nine individual volume densities. The vertical error bar of 35% is within the range of the CLAES extinction accuracies (33-38% at 46 hPa) cited in Table 14 of *Massie et al.* (1996)

Time progresses from January 9 to January 10 from right to left for the observations displayed in Figure 1. An observation was included in Figure 1 if the data point was within 400 km of a parcel trajectory position. Figures 1a and 1b display pairs of aerosol and HNO_3 data which were measured during the same 65 second UARS observation time period, i.e. the volume densities and HNO_3 mixing ratios are simultaneous. The HNO_3 values in Figure 1b are averages of the CLAES and MLS mixing ratios.

In Figure 1 the aerosol is assumed to be Arctic sulfate (H_2SO_4/H_2O droplets) for temperatures greater than 196 K, and assumed to be ternary droplets at temperatures less than 196 K. If the NAT composition is assumed at temperatures less than 196 K, then the volume densities are 20% lower than in the ternary case. The volume density versus temperature graph (not shown), based upon the NAT indices, however, has a visual appearance similar to Figure 1a. The differences in refractive index do not alter the fact that the rise in volume density (with decreasing temperature) in Figure 1a occurs at a temperature less than that expected for a NAT particle. The structure of Figure 1a is controlled primarily by the relationship between temperature and aerosol extinction (e.g., see Figure 5 of *Taylor et al.*, 1994).

Theoretical interpretation

Theoretical equilibrium curves, for NAT, nitric acid dihydrate (NAD) and ternary particles, are presented in Figures 1a-b, and are derived from the programs and data of *Tabazadeh et al.* (1994b), *Carslaw et al.* (1995), and *Worsnop et al.* (1993). Model H_2O values (4-5 ppmv) bracket those observed over Kiruna, Sweeden during the winter of 1992 (see Figure 2 of *Ovarlez and Ovarlez*, 1994). The range of model HNO_3 values, 9-13 ppbv, is based upon the observational range displayed in Figure 1b at temperatures greater than 200 K. Individual MLS and CLAES values (not shown) also varied between 9 and 13 ppbv at temperatures greater than 200 K. Diagonal arrows in panel 1a indicate the most probable (using 11 ppbv HNO_3, 4.5 ppmv H_2O), low (9 ppbv HNO_3, 4.0 ppmv H_2O) and high (13 ppbv HNO_3, 5.0 ppmv H_2O) model limits. The 13 ppbv HNO_3 and 5 ppmv H_2O values yield the largest volume densities. The lower limits for the NAT and NAD curves are shifted by 1K to colder temperatures from the most probable curve temperatures. It is apparent in panels 1a and 1b that increases in volume density are accompanied by decreases in gas phase HNO_3, and that the theoretical curves for the NAT, NAD, and the ternary solutions have different temperature thresholds for uptake of HNO_3, and subsequent increases in the aerosol volume density.

The observed volume densities in Figure 1a, for values less than 2 microns^3 cm^{-3}, are more consistent with the ternary and NAD theory curves than with that of NAT. The volume densities do not increase in magnitude in the 195-196 K range when the volume density is near 0.5 microns^3 cm^{-3}, while the volume densities do increase in magnitude in the 191-193 K range. In panel 1b the averaged HNO_3 values do not decrease in magnitude in the 195-196 K range, as predicted by the NAT curves, while they do decrease in the 191-193 K range, as predicted by the ternary and NAD curves. The volume density and HNO_3 data is consistent with initial PSC growth processes which transform sulfate droplets into ternary droplets or nitric acid dihydrate (NAD) particles, rather than transformation from the sulfate to the nitric acid trihydrate (NAT) phase. This is consistent with previous analyses. *Tabazadeh et al.* (1994a), *Carslaw et al.* (1994), and *Drdla et al.* (1994) used equilibrium ternary models to show that the aerosol growth measured during flight 890124 is consistent with HNO_3 uptake by ternary liquid droplets.

At volumes greater than 3 micron^3 cm^{-3}, the data are more consistent with the ternary and NAT theory curves, since the data points are above the NAD low and high limits. For HNO_3 less than 7 ppbv, all three composition types are consistent with the data. Over the full range of volume density (0.5 to 4 microns^3 cm^{-3}) and HNO_3 (0 to 13 ppbv), the observations and their error bars are consistent with the ternary model values. The larger volume averages (the squares in Figure 1), however, are outside the range given by the ternary model curves.

The data points in Figure 1 do not allow for a simple interpretation (i.e., that only ternary droplets are present). Temperature uncertainties, the presence of several phases along the limb viewing ray paths (see below), the possibility that the volume densities are overestimated, and the possibility that the data is suggestive of a transition from ternary (or NAD) to other forms, complicates the interpretation of Figure 1.

Since the curves in Figure 1b are equilibrium curves, and do not incorporate chemical reactions, a chemical box model is used to investigate the effects of heterogeneous reactions upon the gas phase HNO_3 mixing ratio. The box model uses the SMVGEAR solver (*Jacobson et al.*, 1994), and contains 50 species, 150 reactions, and 16 heterogeneous reactions. The aerosol physical chemistry model (APCM) of *Tabazadeh et al.* (1994b) is used to calculate the equilibrium value of the volume density for the ternary solution droplets, which is used to estimate the area density (assuming a particle density of 2.5 particles/cm^3). For calculations of the NAT particles, the mechanism of *Chipperfield et al.* (1993) is used. The volume and area densities are updated every 15 minutes.

Figure 1c presents theoretical curves of HNO_3 versus temperature. Time is indicated at the top of the figure. The time dependent values in Figure 1c were calculated using the temperatures and times from the parcel trajectory in Plate 1which is closest to the equator. Initial conditions for the calculations were derived from 2d model results, and the UARS observations. The calculations in Figure 1c start with 5 ppmv H_2O, 7 ppbv HNO_3, 2.4 ppbv N_2O_5, 14 ppbv NOy, 1.7 ppbv $ClONO_2$, 1.7 ppbv HCl and 3.5 ppbv Cl_y.

The heterogeneous reactions

$$N_2O_5 + H_2O(\text{aerosol}) \rightarrow 2\ HNO_3 \quad (1)$$

$$ClONO_2 + H_2O(\text{aerosol}) \rightarrow HNO_3 + HOCl \quad (2)$$

$$ClONO_2 + HCl\ (\text{aerosol}) \rightarrow HNO_3 + Cl_2 \quad (3)$$

are influential in determining the gas phase HNO_3 mixing ratio. The "Ternary, all reactions" curve between 0 and 24 hours illustrates that reactions 1-3 enhance polar HNO_3 with a time scale of one day. The other theoretical curves show the results of

the box model with and without heterogeneous reactions. Reaction (1) is the largest source term of gas phase HNO_3. The "Ternary, all reactions" curve is supportive of the conclusion that the decrease of the observed HNO_3 is due to the uptake of gas phase HNO_3 into PSC droplets.

Comparisons with other observations

The January 1992 period over Scandinavia has been studied by ground, aircraft, and satellite instrumentation. A comparison of UARS ClO, $ClONO_2$, HCl, and aerosol data on January 10, 1992 with a three dimensional model is discussed by *Geller et al.* (1995).

Airborne FTIR emission observations, on January 9, of low HNO_3 column amounts west of Norway (67.6°N, 9.5°E) by *Höpfner et al.* (1996) are consistent with NAT particles, i.e. the observed HNO_3 column and the ECMWF temperature profile are more consistent with the theoretical equilibrium HNO_3 column for NAT, than with that of the ternary solution. It is interesting to note that the lowest HNO_3 mixing ratios in Figure 1b are within 600 km of the location of the *Höpfner et al.* observations.

Schäfer et al. (1994) report lidar observations at Andoya Island (69°N, 16°E), which is located along the coast of Norway, on January 5, 8, 9 and 1992. The depolarization and perpendicular backscatter data on January 9 support the presence of nonspherical PSC particles at altitudes above 20 km, and spherical particles below 20 km. It is commonly held that nonspherical particles are solid "Type Ia NAT" particles, while spherical particles are liquid "Type Ib Ternary" droplets. Though the data presented in Figure 1b apply to the pressure range between 46 and 68 hPa, for which the lidar reports ternary droplets, the satellite limb-viewing ray path does pass through altitudes for which both ternary and NAT particles are present.

Acknowledgments. This work was funded by the NASA UARS Guest Investigator Program by grant S-12899-F. The National Center for Atmospheric Research (NCAR) is sponsored by the National Science Foundation.

References

Carslaw, K. S., *et al.*, Stratospheric aerosol growth and HNO_3 gas phase depletion from coupled HNO_3 and water uptake by liquid particles, *Geophys. Res. Lett.*, *21*, 2479-2482, 1994.

Carslaw, K. S., *et al.*, An analytic expression for the composition of aqueous HNO_3-H_2SO_4 stratospheric aerosols including gas phase removal of HNO_3, *Geophys. Res. Lett*, *22*, 1877-1880, 1995.

Chipperfield, M. P., D. Cariolle, P. Simon, R. Ramaroson, and D. J. Lary, A three-dimensional modeling study of trace species in the Arctic lower stratosphere during winter 1989-1990, *J. Geophys. Res.*, *98*, 7199-7218, 1993.

Deshler, T., *et al.*, Balloonborne measurements of Pinatubo aerosol during 1991 and 1992 at 41° N: Vertical profiles, size distribution, and volatility, *Geophys. Res. Lett.*, *20*, 1435-1438, 1993.

Drdla, K., *et al.*, Analysis of the physical state of one Arctic polar stratospheric cloud based on observations, *Geophys. Res. Lett.*, *21*, 2475-2478, 1994.

Dye, J. E., *et al.*, Particle Size Distributions in Arctic Polar Stratospheric Clouds, Growth and Freezing of Sulfuric Acid Droplets, and Implications for Cloud Formation, *J. Geophys. Res.*, *97*, 8015-8034, 1992.

Geller, M., *et al.*, UARS PSC, $ClONO_2$, HCl, and ClO measurements in early winter: Additional verification of the paradigm for chlorine activation, *Geophys. Res. Lett.*, *22*, 2937-2940, 1995.

Höpfner, M., *et al.*, Evidence for the removal of gaseous HNO_3 inside the Arctic polar vortex in January 1992, *Geophys. Res. Lett.*, *23*, 149-152, 1996.

Jacobson, M. Z., and R. P. Turco, SMVGEAR: A sparse-matrix vectorized Gear code for atmospheric models, *Atmos. Environ.*, *28A*, 273-284, 1994.

Kumer, J. B., *et al.*, Comparison of correlative data with nitric acid data version v7 from the Cryogenic Limb Array Etalon Spectrometer (CLAES) instrument deployed on the NASA Upper Atmosphere Research Satellite (UARS), *J. Geophys. Res.*, *101*, 9621-9656, 1996.

Lambert, A., *et al.*, Validation of aerosol measurements by the Improved Stratospheric and Mesospheric Sounder, *J. Geophys. Res.*, *101*, 9811-9830, 1996.

Larsen, N., *et al.*, Balloonborne backscatter observations of type 1 PSC formation: Inference about physical state from trajectory analysis, *Geophys. Res. Lett.*, *23*, 1091-1094, 1996.

Manney, G. *et al.*, Comparison of U. K. Meterological Office and U. S. National Meterological Center stratospheric analyses during northern and southern winter, *J. Geophys. Res.*, *101*, 10311-10334, 1996.

Massie, S. T., *et al.*, Validation Studies Using Multi-wavelength CLAES Observations of Stratospheric Aerosol, *J. Geophys. Res.*, *101*, 9757-9733, 1996.

Ovarlez, J., H. and H. Ovarlez, Stratospheric water vapor content evolution during EASOE, *Geophys. Res. Lett.*, *21*, 1235-1238. 1994.

Santee, M. L., *et al.*, Polar vortex conditions during the 1995-96 Arctic winter: MLS ClO and HNO_3, submitted to *Geophys. Res. Lett.*, 1996.

Schäfer, *et al.*, Lidar observations of polar stratospheric clouds at Andoya, Norway, in January 1992, *Geophys. Res. Lett.*, *21*, 1307-1310, 1994.

Tabazadeh, A., *et al.*, A study of Type I polar stratospheric cloud formation, *Geophys. Res. Lett.*, *21*, 1619-1622, 1994a.

Tabazadeh, A., *et al.*, A model for stydying the composition and chemical effects of stratospheric aerosols, *J. Geophys. Res.*, *99*, 12897-12914, 1994b.

Tabazadeh, A., *et al.*, The presence of metastable HNO_3/H_2O solid phases in the stratosphere inferred from ER-2 data, *J. Geophys. Res.*, *101*, 9071-9078, 1996.

Taylor, F. W., et al., Properties of Northern Hemisphere Polar Stratospheric Clouds and Volcanic Aerosol in 1991/92 from UARS/SAMS Satellite Measurements, *J. Atm. Sci.*, *51*, 3019-3026, 1994.

Worsnop, *et al.*, Vapor Pressures of Solid Hydrates of Nitric Acid: Implications for Polar Stratospheric Clouds, *Science*, *259*, *71-74*, 1993.

Steven T. Massie, James E. Dye, Darrel Baumgardner, William J. Randel, Fei Wu, XueXi Tie, Liwen Pan, Francois Figarol, and Guy. P. Brasseur (National Center for Atmospheric Research, PO Box 3000, Boulder, CO, 80307)

Michelle L. Santee and William G. Read (Jet Propulsion Laboratory, 4800 Oak Grove Drive, Pasadena, CA, 91109)

Roy G. Grainger and Alyn Lambert (Atmospheric, Oceanic and Planetary Physics, Oxford University, Oxford, UK)

John L. Mergenthaler (Lockeed-Martin Palo Alto Research Laboratory, Dept 91-20, 3251 Hanover Street, Palo Alto, CA,94304)

Azadeh Tabazadeh (NASA-Ames Research Center, Moffett Field, CA, 94035-1000)

(Received: August 23, 1996; revised January 24, 1997; accepted:January 27, 1997.)